Received 30 September 2025
Revised 29 November 2025
7 December 2025
15 December 2025
Accepted 23 December 2025

Weibull option Greeks for managing residual value risk in automotive finance

Seok Bin Ko
College of Economics and Business Administration, Cheongju University, Cheongju, South Korea

Abstract
This study proposes a Weibull-based framework for managing residual value (RV) risk in automotive leasing and demonstrates its direct applicability to key business decisions. Unlike lognormal option models, the Weibull specification captures the asymmetric and fat-tailed nature of used-car values, or more broadly, depreciating asset values, enabling finance companies to quantify exposures more realistically. The framework embeds option-theoretic sensitivities into five operational metrics, including the offset budget, offer-timing score, volatility guardrail, scale guardrail and composite distributional alert, and applies them to Hyundai Sonata transactions in South Korea. The results show that these tools support managerial use by guiding incentive allocation, customer outreach timing and guarantee adjustments in response to rate and volatility shocks. Robustness checks confirm the stability of the metrics under bootstrap sampling and rolling parameter estimates, as well as the consistency of the Weibull-based sensitivities across vehicle models relative to lognormal and gamma benchmarks. Year-by-year tests spanning turbulent COVID-era conditions through the subsequent normalization period further show that the Weibull specification maintains a reliably strong fit. The study concludes that the framework provides practical value for auto finance companies and offers fertile directions for future work on time-varying models, as well as opportunities to extend the approach to industries where extreme, outlier-driven losses are central to risk management.

Keywords Residual value risk, Weibull distribution, Option pricing, Automotive finance, Lease retention strategy
Paper type Research article

1. Introduction

The automobile leasing market has expanded substantially across major economies over the past 2 decades. In the United States, Federal Reserve statistics document a steady rise in outstanding lease balances, underscoring the increasing role of leasing in retail auto finance (Federal Reserve Bank of St. Louis, 2025). Similar growth patterns have been observed in South Korea, where leasing has gained market share relative to traditional installment financing (Mordor Intelligence, 2025), and in Europe, where leasing and rental penetration continue to shape consumer mobility trends (Eurofinas, 2024).

For both captive and independent finance companies, leasing typically generates higher expected returns than installment loans. Data from South Korea's Financial Supervisory Service indicate that leases deliver markedly greater profitability for the country's three major auto finance companies (see Table 1). However, inadequate management of residual value (RV) risk can lead to substantial losses. Chrysler's experience in the early 2000s, when depressed used-car prices prompted large write-offs on returned vehicles, remains a widely cited example of the consequences of mispriced RV guarantees (Belzowski, 2009).

JEL Classification — G12, G13, G17

Financial interests: The author(s) have no competing interests to declare that are relevant to the content of this article.

Journal of Derivatives and Quantitative Studies: 선물연구
Vol. 34 No. 2, 2026
pp. 128-142
Emerald Publishing Limited
e-ISSN: 2713-6647
p-ISSN: 1229-988X
DOI 10.1108/JDQS-09-2025-0065

Table 1. Major Korean auto finance companies' returns by asset type. (unit: million USD)

	Asset type	Average balance	Returns	Annual return rate
Hyundai Capital	Leases	6,023	690	22.92%
	Loans	12,498	306	4.89%
KB Capital	Leases	3,083	230	14.94%
	Loans	2,135	72	6.76%
Lotte Capital	Leases	1,984	159	16.06%
	Loans	29	0.7	4.84%

Note(s): All amounts in Korean won (KRW) are converted into U.S. dollars (USD) using the prevailing exchange rate of 1,293.5 KRW per USD. The final sample period spans from January 1 to June 30, 2023. Data are obtained from the Financial Supervisory Service of Korea (https://dart.fss.or.kr)

These episodes have motivated a substantial body of research that models RV risk using financial option theory (Gamba and Rigon, 2008; Giaccotto *et al*., 2007; Li and You, 2022; McConnell and Schallheim, 1983; Miller, 1995; Oppenheimer, 2002; Trigeorgis, 1996). Although option-theoretic models provide elegant treatments of embedded guarantees, their practical adoption has been limited because used-car values violate core assumptions of lognormal pricing frameworks. Specifically, RV dynamics do not display square-root-of-time scaling, empirical distributions are left-skewed with bounded upside, and downside tails are considerably heavier than implied by lognormality (Ko, 2025). These structural features often lead lognormal-based models to misprice RV exposures.

While earlier studies have considered non-lognormal or heavy-tailed depreciation processes in reliability engineering and equipment leasing (Park and Padgett, 2006; Ye and Chen, 2014), the implications for used-car RVs remain underexplored despite their pronounced asymmetry and bounded support. To address this gap, Ko (2025) introduced a Weibull-based put option pricing framework specifically tailored to depreciating assets. The Weibull distribution captures the skewed and truncated nature of RV outcomes, producing risk measures that align more closely with observed data. Empirical evidence from South Korean used-car transactions shows that the Weibull specification outperforms lognormal benchmarks and provides a coherent basis for quantifying RV losses. Ko (2025) also demonstrated its relevance for risk management, regulatory capital planning, and funding-cost negotiations.

Yet, the managerial implications of this framework have largely focused on risk measurement rather than strategic decision-making. In practice, leasing serves not only as a financing product but also as a critical lever for new-vehicle sales, particularly for captive finance companies. Retention efforts, such as contacting lessees within three months of maturity to encourage renewal or repurchase, often yield higher returns and lower acquisition costs than conquest sales, according to internal sources at a major South Korean captive. Effective management of lease maturity, therefore, enhances both RV risk control and customer lifetime value for manufacturers.

This study extends Ko's (2025) Weibull-based model by embedding it within a broader strategic framework for leasing operations. We examine how finance companies can adjust product design, customer engagement, and risk-adjusted pricing in response to shifts in interest rates and market volatility. Central business questions include how to attract customers in rising-rate environments, whether the prevailing three-month contact window is optimal for lease retention or repurchase, and how volatility should influence product development. To address these questions, we derive and implement Weibull-based option Greeks that translate RV risk into operationally meaningful sensitivity measures. Our empirical application uses Hyundai Sonata transactions with up to 60 aging months, reflecting the practical maximum lease horizon in South Korea, and demonstrates how the proposed metrics can support strategic and managerial decision-making.

2. Methodology

To ensure theoretical consistency in option valuation, the terminal residual value distribution must be evaluated under the risk-neutral measure Q. Let S_T denote the residual value at maturity. Under the physical measure P, we assume that S_T follows a Weibull distribution with scale $\theta > 0$ and shape $\delta > 0$.

The risk-neutral measure is constructed so that the distribution of S_T under Q remains within the same Weibull family. The empirical shape parameter δ is preserved, and only the scale parameter is adjusted in order to satisfy the no-arbitrage condition. Appendix A provides the formal change of measure. In this construction, the Radon-Nikodym derivative is defined by the ratio of the physical and risk-neutral Weibull densities. This approach delivers a valid equivalent martingale measure and does not rely on exponential tilting or any additional closure property of the Weibull family.

The invariance of δ is an explicit modeling choice. From an economic perspective, the shape parameter reflects structural features of used-vehicle depreciation, including heterogeneity in condition, mileage accumulation, and segment-specific aging effects. These characteristics arise from the physical depreciation process and are not related to investor risk preferences. For this reason, δ is treated as a structural parameter that remains unchanged when moving from the physical measure to the risk-neutral measure.

Under the risk neutral specification, the scale parameter adjusts to satisfy $E_Q[S_T] = S_0 e^{rT}$. The resulting risk-neutral scale parameter θ_Q follows directly from the mean of a Weibull distribution, and its derivation is also included in Appendix A. All pricing expressions are evaluated using (θ_Q, δ), and θ_Q is denoted simply as θ hereafter.

The guaranteed residual risk in a car lease can be represented as a put option on the residual value. Consider a lease with maturity T, risk-free rate r, and guaranteed residual value K. The terminal payoff is $P_T = (K - S_T)^+$, where S_T denotes the residual value at maturity. Under the risk-neutral measure, the present value is:

$$P_0 = e^{-rT} E_Q[(K - S_T)^+].$$

Following Ko (2025), we assume S_T follows a Weibull distribution with scale $\theta > 0$ and shape > 0. With the reparameterization $\beta = (1/\theta)^\delta > 0$, Ko's pricing formula is converted to:

$$P_0 = e^{-rT} K F_{\text{Weibull}}(K;\, \theta, \delta) - S_0 \gamma\left(1 + 1/\delta, (K/\theta)^\delta\right) / \Gamma(1 + 1/\delta), \tag{1}$$

where S_0 is the initial asset value, $F_{\text{Weibull}}(\cdot;\, \theta, \delta)$ is the Weibull CDF, $\gamma(\cdot, \cdot)$ is the lower incomplete gamma function, and $\Gamma(\cdot)$ is the gamma function. Both K and S_0 are deterministic quantities estimated via nonlinear regression and therefore remain explicit in the pricing expression. For clarification, S_0 is the present value of an estimated residual value at maturity.

2.1 Interest-rate and maturity sensitivities

Differentiating Ko (2025)'s formula with respect to the discount factor yields closed-form expressions for rho and theta. The interest-rate sensitivity is:

$$\rho = \frac{\partial P_0}{\partial r} = -T e^{-rT} K F_{\text{Weibull}}(K;\, \theta, \delta), \tag{2}$$

which is strictly negative for put options, indicating that higher rates lower option values. This effect provides a natural hedge for finance companies, as the decline in option values partially offsets the increased burden on customers when rates rise.

The maturity sensitivity is:

$$\Theta = \frac{\partial P_0}{\partial T} = -re^{-rT} K F_{\text{Weibull}}(K;\, \theta, \delta), \tag{3}$$

which captures the decay of time value as the lease approaches expiration. For simplicity, we assume a constant interest rate. This measure enables the validation of industry practice, which initiates repurchase offers three months prior to maturity, by demonstrating whether the steepest time-value loss indeed occurs within that window.

2.2 Volatility sensitivity

Volatility is more complex because the Weibull distribution is governed by the scale θ and shape δ. To obtain an interpretable measure, we use the coefficient of variation (CV), defined as the ratio of the standard deviation to the mean. For the Weibull distribution (Weibull, 1951):

$$\mu = \theta \cdot \Gamma\left(1 + \frac{1}{\delta}\right), \sigma^2 = \theta^2 \left[\Gamma\left(1 + \frac{2}{\delta}\right) - \Gamma\left(1 + \frac{1}{\delta}\right)^2\right] \tag{4}$$

so that:

$$CV = \frac{\sigma}{\mu} = \frac{\sqrt{\theta^2 \left[\Gamma(1 + 2/\delta) - \Gamma(1 + 1/\delta)^2\right]}}{\theta \cdot \Gamma(1 + 1/\delta)} = \sqrt{\frac{\Gamma(1 + 2/\delta)}{\Gamma(1 + 1/\delta)^2} - 1}. \tag{5}$$

Because θ cancels out, the coefficient of variation depends only on the shape parameter δ. The CV-based Vega is the sensitivity of the option's value to changes in CV. The following lemma provides a convenient representation.

Lemma 1. (Chain rule representation of CV-based Vega). Let $\mathrm{P}_0 = \mathrm{P}_0(\mathrm{r}, \mathrm{T}, \theta, \delta)$ denote the Weibull option price of Ko (2025), and let $\mathrm{CV} = \mathrm{CV}(\delta)$ denote the coefficient of variation of the Weibull distribution. Then, the CV-based Vega satisfies

$$\upsilon_{CV} = \frac{\partial P_0}{\partial CV} = \frac{\partial P_0 / \partial \delta}{dCV / d\delta} \tag{6}$$

Proof. The shape parameter δ affects the option value through the coefficient of variation, CV(δ). Hence, the option price can be regarded as a function of CV rather than δ itself. Applying the chain rule,

$$\frac{\partial P_0}{\partial \delta} = \frac{\partial P_0}{\partial CV} \cdot \frac{dCV}{d\delta},$$

and rearranging yields the stated result. For computation, $\partial P_0 / \partial \delta$ is obtained by differentiating Ko (2025)'s formula with respect to δ while holding (r,T,θ) fixed, and $dCV/d\delta$ follows from the closed-form expression for CV in (6). □

This lemma shows that the CV-based Vega can be obtained without reparameterizing the option price in terms of CV. The measure remains robust and interpretable because it links option values directly to the relative dispersion of residual values.

In the meantime, sensitivity to level shifts is governed by the scale parameter:

$$v_\theta = \frac{\partial P_0}{\partial \theta} \tag{7}$$

which reflects how option values respond when the distribution shifts upward or downward with θ. Let $x = (K/\theta)^\delta$. Using

$$F(K;\, \theta, \delta) = 1 - e^{-x} = 1 - e^{-(K/\theta)^\delta},$$

$$\frac{\partial F}{\partial \theta} = -\frac{\delta}{\theta}\left(\frac{K}{\theta}\right)^\delta e^{-x},$$

$$\frac{\partial}{\partial \theta}\gamma\left(1 + \frac{1}{\delta}, x\right) = -\frac{\delta}{\theta}\left(\frac{K}{\theta}\right)^{\delta+1} e^{-x},$$

Hence, we obtain the closed form:

$$v_\theta = \frac{\partial P_0}{\partial \theta} = -e^{-rT} K \frac{\delta}{\theta}\left(\frac{K}{\theta}\right)^\delta e^{-\left(\frac{K}{\theta}\right)^\delta} + S_0 \frac{\delta}{\theta}\left(\frac{K}{\theta}\right)^{\delta+1} \frac{e^{-(K/\theta)^\delta}}{\Gamma(1 + 1/\delta)}. \tag{8}$$

A larger θ shifts the distribution right. The first term pulls $\partial P_0/\partial\theta$ down, and the second pushes it up. The net sign is state-dependent and will be quantified empirically.

2.3 Composite vega index

Although the CV-based Vega captures shape-driven dispersion risk and the scale sensitivity v_θ reflects level shifts, these two measures do not fully capture all distributional changes. Tail fattening or skewness asymmetries, for example, may not be detected by either measure in isolation. To address this limitation, we define a composite Vega index that integrates sensitivities to both the scale and shape parameters:

$$\mathcal{V} = \omega_\theta \frac{v_\theta}{P_0}\frac{\Delta\theta}{\theta} + \omega_\delta \frac{v_\delta}{P_0}\frac{\Delta\delta}{\delta}, \tag{9}$$

where $v_\theta = \partial P_0/\partial\theta$ and $v_\delta = \partial P_0/\partial\delta$. The weights ω_θ and ω_δ reflect the relative contribution of scale and shape changes to option value variability. This index extends the notion of Vega beyond dispersion alone, providing a supplementary tool for identifying asymmetric shocks or structural shifts in residual value distributions.

3. Empirical analysis

3.1 Implementation framework

The empirical analysis uses transaction-level records for Hyundai Sonata units originally sold before 2023 and traded in the secondary market during 2023. We restrict the horizon to 60 months, the modal lease maturity in South Korea. This differs from the longer horizons in earlier work (Ko, 2025) but reflects domestic market practice, where nearly all leases mature within 60 months. Detailed lease information was obtained from Hyundai Capital, and the transaction data were sourced from the Ministry of Land, Infrastructure and Transport (MOLIT), Republic of Korea.

For analytical consistency, the main results focus on the Sonata dataset, with three additional models (K5, Santa Fe, and Sorento) used for external validation. These high-volume vehicles cover both sedan and SUV segments, and applying identical filtering criteria ensures comparability. Appendix B shows that Weibull parameters and key sensitivity metrics remain stable across models.

Before estimation, we implement a structured cleaning pipeline. First, employee-discount units are identified using *k*-means clustering (Rousseeuw, 1987; Steinley and Brusco, 2007). Sonata trims include Low, Medium, High, and Premium, with Medium and High accounting for about 80% of sales and a 13 to 14% price range. Hyundai employees, however, receive discounts of 16–30% depending on tenure, and those with more than 25 years of service may obtain a permanent 30% discount every two years. These institutional discounts form a distinct price cluster. The *k*-means procedure effectively isolates this group, and the silhouette scores in Appendix B confirm clear separation.

Second, we detect remaining idiosyncratic outliers using an Extended Isolation Forest (Hariri *et al*., 2019). The contamination rate is selected by cross-validation to maintain a stable flagged share while preserving the core distribution.

Third, we exclude residual values above 100% or below 5%. Values near or below 5% arise almost entirely from severe accident or flood damage, losses that are insured rather than borne by lessors. Conversely, residuals above 100% are attributable to data entry errors, post-repair resale cases, or idiosyncratic owner pricing and are not relevant for automotive finance. Removing these observations follows industry convention and maintains the focus on economically meaningful lease-end risks.

After preprocessing, we fit a Weibull distribution by maximum likelihood for each month t (see Appendix B), obtaining $\widehat{\theta}_t$ and $\widehat{\delta}_t$. Given the depth of monthly data, δ is estimated at a lower frequency, either annually or with smoothing, while θ varies monthly to capture short-run changes. The guaranteed residual K_t and initial value $S_{0,t}$ are derived from deterministic nonlinear regression consistent with portfolio valuation practice and remain explicit in the pricing formula.

To evaluate distributional adequacy, we compare the Weibull specification with lognormal and gamma alternatives using the filtered and unfiltered samples. All models are estimated by maximum likelihood, and goodness-of-fit statistics are computed. The Weibull distribution consistently produces the lowest AIC and BIC values and the smallest Kolmogorov-Smirnov distances, and QQ plots show only mild lower-tail deviations. These findings support the use of the Weibull specification for option valuation. Detailed comparisons are presented in Appendix C.

Using these inputs, we compute Ko's (2025) Weibull option value at $T = 60$ months and the associated Greeks $(\rho_t, \Theta_t, \upsilon_{CV}, \upsilon_\theta)$. We also construct a Composite Vega Index V that combines scale and shape sensitivities using operational weights calibrated from observed variation in option values. These measures form the basis for the scenario experiments and policy interpretations that follow.

3.2 Estimation strategy and identification

Each observation is a used-car transaction observed in 2023. Let $\lambda \in [1, 60]$ denote the month-in-service at its 2023 transaction date. For a 60-month lease horizon, the remaining maturity for that observation is $\Delta \equiv \max(60 - \lambda, 0)$. For month t, we evaluate the put option price:

$$P_{0,t} = P_0(r_t, T = 60, \widehat{\theta}_t, \widehat{\delta}_t, K_t, S_{0,t})$$

using the deterministic K_t, $S_{0,t}$ fits described in Section 3.1. Greeks are then computed directly as defined in Section 2.

$$\rho_t = -T \cdot e^{-rT} K_t F_{\text{Weibull}}(K;\, \theta, \delta) \tag{10}$$

$$\Theta_t = -r_t e^{-rT} K_t F_{\text{Weibull}}(K;\, \theta, \delta) \tag{11}$$

$$\upsilon_{CV,t} = \frac{(\partial P_0/\partial\delta)_t}{(dCV/d\delta)_{\widehat{\delta_t}}},\, CV(\delta) = \sqrt{\frac{\Gamma(1+2/\delta)}{\Gamma(1+1/\delta)^2} - 1} \tag{12}$$

$$\upsilon_{\theta,t} = \frac{\partial P_0}{\partial\theta}\bigg|_{\left(r_t, T=60, \widehat{\theta}_t, \widehat{\delta}_t, K_t, S_{0,t}\right)}. \tag{13}$$

Finally, the composite vega index consolidates scale and shape sensitivities:

$$\mathcal{V}_t = \omega_\theta \frac{\upsilon_{\theta,t}}{P_{0,t}} \frac{\Delta\theta}{\theta} + \omega_\delta \frac{\upsilon_{\delta,t}}{P_{0,t}} \frac{\Delta\delta}{\delta}, \tag{14}$$

where $\upsilon_{\theta,t} = \partial P_0/\partial\theta$ and $\upsilon_{\delta,t} = \partial P_0/\partial\delta$. The operational weights ω_θ and ω_δ are calibrated from the historical decomposition of option-value variability into scale-vs shape-driven components. When history is short, we begin with $\omega_\theta = 1, \omega_\delta = 0$ and gradually introduce ω_δ as stability improves.

3.3 From Greeks to KPIs: mapping to operating levers

The first operating metric is the offset budget (OB), which provides guidance for handling rate shocks. When interest rates increase by $\Delta r > 0$, customer affordability deteriorates. At the same time, the value of the embedded put option declines by $-\rho_t \Delta r$, creating an economic offset that the finance company can use as a buffer. This offset budget can be expressed as:

$$OB_t(\Delta r) \approx -\rho_t \Delta r = \left[T \cdot e^{-rT} K F_{\text{Weibull}}(K;\, \theta, \delta)\right] \Delta r \tag{15}$$

In practice, this budget can be deployed to fund incentive credits or to permit a marginally higher residual guarantee K while keeping the firm's risk-adjusted economics neutral.

A second metric is the offer-timing score (OTS), which links time decay to customer outreach. Time decay captures how fast the protection embedded in the put option erodes as maturity approaches. We define from Eq. (11):

$$\Theta_t = -r_t e^{-rT} K_t F_{\text{Weibull}}(K_t;\, \widehat{\theta}_t, \widehat{\delta}_t), \tag{16}$$

and the OTS as the ratio of instantaneous time decay to the current option value:

$$OTS_t = \frac{|\Theta_t|}{P_{0,t}} = \frac{r_t e^{-rT} K_t F_{\text{Weibull}}(K_t;\, \widehat{\theta}_t, \widehat{\delta}_t)}{P_{0,t}} = \frac{r_t}{T} \frac{|\rho_t|}{P_{0,t}}, \tag{17}$$

where ρ_t is the interest-rate sensitivity from Eq. (10). A high realized OTS suggests that the erosion of option value is steep for a given group of customers, thereby flagging segments where earlier-than-usual outreach (conventional "three months prior to maturity" rule) would be justified.

The third operating metric is the volatility guardrail (VG), which is derived from the CV-Vega sensitivity. When dispersion in used-car values increases by $\Delta CV > 0$, the expected put-cost rises by $\upsilon_{CV,t}\Delta CV$. To keep products stable under such conditions, guardrails can be imposed on either the guaranteed residual value or incentive spending. Formally,

$$\Delta K_t^{\max} \approx -\alpha \frac{\upsilon_{CV,t}}{\partial P_0/\partial K}\Delta CV, \Delta Incentive_t^{\max} \approx -\beta \upsilon_{CV,t}\Delta CV \tag{18}$$

where $\alpha, \beta \in [0,1]$ reflect the institution's risk appetite. The derivative $\partial P_0/\partial K = e^{-r_t T} F_{Weibull}(K_t; \widehat{\theta}_t, \widehat{\delta}_t)$ governs how residual guarantees feed into option value, ensuring that adjustments remain economically consistent.

A fourth operating metric is the scale guardrail (SG), based on the scale sensitivity.

$\upsilon_{\theta,t}$. While CV-Vega captures shape-driven dispersion shocks, the scale parameter θ governs the overall level of residual values. A shock $\Delta\theta/\theta \neq 0$ alters option values according to $\upsilon_{\theta,t} = \partial P_0/\partial\theta$. Guardrail rules translate this into operational limits:

$$\Delta K_t^{\max} \approx -\eta_K \frac{\upsilon_{\theta,t}}{\partial P_0/\partial K}\frac{\Delta\theta}{\theta}, \Delta Incentive_t^{\max} \approx -\eta_I \upsilon_{\theta,t}\frac{\Delta\theta}{\theta}, \tag{19}$$

where $\eta_K, \eta_I \in [0,1]$ reflects tolerance to level shocks. A positive scale shift allows more generous guarantees or lower incentives, while a negative shift requires tightening terms.

Finally, we introduce the Composite Distributional Alert (CDA), which supplements CV-based and scale-based monitoring by consolidating both dimensions of distributional change into a single trigger. The composite index $\mathcal{V}_t$, defined in (14), aggregates sensitivities to scale θ and shape δ with operational weights calibrated to the historical decomposition of option-value variability.

An alert is triggered whenever $\mathcal{V}_t > \tau$, where τ is a model-specific threshold such as the 95th percentile of historical values. To interpret the signal, the composite index can be decomposed into contributions:

$$C_{\theta,t} = \omega_\theta \frac{\upsilon_{\theta,t}}{P_{0,t}}\frac{\Delta\theta}{\theta}, C_{\delta,t} = \omega_\delta \frac{\upsilon_{\delta,t}}{P_{0,t}}\frac{\Delta\delta}{\delta}, \tag{20}$$

with attribution shares $\phi_{\theta,t} = |C_{\theta,t}|/(|C_{\theta,t}|+|C_{\delta,t}|)$, and $\phi_{\delta,t} = 1 - \phi_{\theta,t}$. When the CDA threshold is breached, the attribution shares indicate whether risk is scale-driven, shape-driven, or mixed.

Economically, scale and shape shocks represent two distinct sources of resale-value risk. A scale shock $(\Delta\theta/\theta)$ shifts the entire distribution, immediately affecting valuations and creating mark-to-market exposure. A shape shock $(\Delta\delta/\delta)$ leaves current prices unchanged but alters depreciation curvature, influencing how value erodes as vehicles age and generating a gradual, structural form of risk.

These differences translate into operational responses. Scale-driven alerts call for adjustments to residual guarantees K or incentive guardrails, while shape-driven alerts motivate tail-oriented measures such as targeted buyout credits. Mixed signals require balanced use of both levers. The CDA therefore provides an integrated operational KPI that captures distributional shifts not fully revealed by CV or scale sensitivities alone.

4. Results

4.1 Experiments for business issues

We now examine how the five operating metrics apply to practical lease-management problems. The put option price serves as the analytical baseline for the scenario experiments that follow.

4.1.1 Experiment A: rate shock and offset budget (OB). Suppose external market rates rise by Δr while the customer-facing interest rate remains fixed. The affordability gap corresponds to the annuity cost of Δr at a 60-month horizon. The embedded put value falls by

$$-\rho_t \Delta r = \left[T \cdot e^{-rT} K F_{\text{Weibull}}(K;\, \theta, \delta)\right] \Delta r,$$

which defines the offset budget

$$OB_t(\Delta r) = \left[T \cdot e^{-rT} K F_{\text{Weibull}}(K;\, \theta, \delta)\right] \Delta r.$$

This budget can be redeployed as incentive credits or used to adjust residual guarantees. If the affordability gap exceeds the offset, the guarantee K is modified using $(\partial P_0 / \partial K)$ to restore neutrality. As shown in Appendix B, a 100-basis-point increase in the 2023 Sonata case yields an offset budget of KRW 280,838, which can lower customer financing costs or allow captive finance companies to raise guaranteed residual values while maintaining economic neutrality.

4.1.2 Experiment B: offer-timing score (OTS) and outreach timing. The timing of lessee outreach for repurchase is a central managerial decision in auto finance. Cohorts with shorter maturities T, higher strikes K_t, or greater Weibull mass at K_t exhibit higher OTS, indicating faster erosion of embedded protection.

Rather than relying on the conventional three-month rule, outreach can be advanced when realized OTS exceeds a calibrated threshold. We adopt the empirical 75th percentile ($\tau = 0.0194$), which limits false positives while capturing periods of accelerated decay. Nearby cutoffs at the 70th and 80th percentiles (0.0177, 0.0223) shift the trigger window by only one or two months and preserve cohort rankings, indicating that the rule is stable across reasonable quantile choices.

For the 2023 Sonata sample as shown in Figure 1, outreach should be advanced from the usual three-month window to roughly six months before maturity, with further intensification near month 24 where OTS exceeds the threshold. Cohorts highlighted in green show how static timing rules miss these high-pressure periods, demonstrating the operational value of OTS-based triggers.

The figure reports bucket-level rolling mean monthly $OTS = |\Theta| / P_0$ across remaining months Δ (three-month cohorts, center-aligned). Cohorts with $\Delta \leq 3$ are labeled contact-now. For $\Delta > 3$, early outreach is triggered when the rolling mean satisfies $OTS_{\text{roll\_mean}} \geq \tau$. The dotted line marks the threshold $\tau = 0.0194$, the empirical 75th percentile of cohort-level OTS.

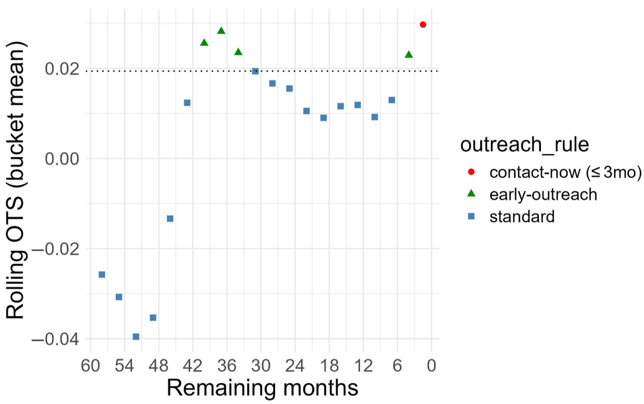

Figure 1. Outreach recommendation: three-month cohorts

4.1.3 Experiment C: dispersion shocks and volatility guardrail (VG). We simulate shocks to cross-sectional dispersion and implement the VG rules, separately for the strike-price channel K governed by α (see Figure 2a), and the incentive channel governed by β (see Figure 2b). For K, a dispersion increase of $\Delta CV = 0.10$ leads to substantial tightening: with $\alpha = 1.0$, the maximum guarantee cut is about KRW 1.4 million, with $\alpha = 0.5$, it is about KRW 0.7 million, and with $\alpha = 0.25$, it is about KRW 0.35 million.

On the incentive side, the same ΔCV shock passes through proportionally via β. With $\beta = 1$, the cap on incremental incentives is about KRW 0.5 million, with $\beta = 0.5$, it is about KRW 0.25 million, and with $\beta = 0.25$, it is about KRW 0.12 million. These results show that VG responses scale linearly with ΔCV but are shaped by the policy parameters α and β. Management can therefore adjust guarantees, incentives, or both to stabilize products when dispersion widens.

Panel (a) shows the change in the maximum feasible strike price $\Delta K_{\max}$ and Panel (b) the change in maximum feasible incentives as the coefficient of variation ΔCV increases. The CV, defined as the standard deviation divided by the mean, provides a scale-free volatility measure. Both panels show that higher volatility sharply reduces allowable adjustments, reflecting greater mispricing risk in unstable conditions. The policy parameters α and β determine the strictness of the guardrails, with larger values imposing tighter limits. Together, the panels illustrate how the dual guardrail mechanism constrains strike prices and incentives in response to volatility shocks, keeping product design within risk-tolerant bounds.

4.1.4 Experiment D: level shocks and scale guardrail (SG). Level shocks to the Weibull scale parameter θ shift the entire residual-value distribution, and the scale guardrail converts these shifts into systematic adjustments of strike prices and incentives. Figure 3a shows that a positive level shock $(\Delta\theta/\theta > 0)$ raises the maximum feasible strike, while a negative shock lowers it. The size of the adjustment scales with the intensity parameter η_K: for a 10% shock, $\Delta K^{\max}$ changes by about four to five thousand KRW when $\eta_K = 1$, with proportionally smaller effects at $\eta_K = 0.5$ or 0.25. Figure 3b shows the same pattern on the incentive side, where η_I governs the response. A 10% shock changes the maximum incentive by roughly one to one and a half thousand KRW at $\eta_I = 1$.

Panel (a) reports how relative changes in the Weibull scale parameter $(\Delta\theta/\theta)$ affect the maximum feasible strike price $\Delta K_{\max}$, and Panel (b) shows the corresponding effect on maximum incentives. Upward scale shifts increase feasible adjustments, while downward shifts reduce them. The policy parameters η_K and η_I govern the strictness of the guardrail. Overall, the panels illustrate how scale guardrails regulate strike and incentive levels under varying distributional conditions.

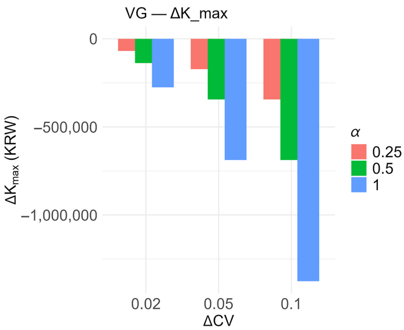

(a)

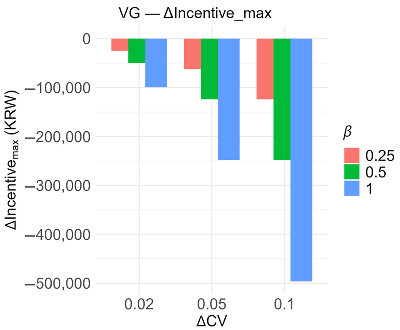

(b)

Figure 2. Volatility guardrail for strike price and incentive adjustment

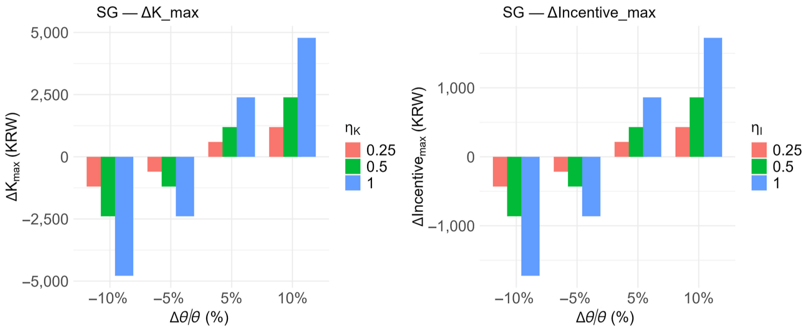

(a) **(b)**

Figure 3. Scale guardrail for strike price and incentive adjustment

Although these KRW amounts are modest in absolute terms, their normalized magnitudes are economically meaningful. Using an internal target profit rate of 8.5% and a discount rate of 5.0%, a vehicle price of 28,080,000 KRW with a guaranteed RV rate of 55.1% implies a monthly lease payment of about 368,000 KRW for a 60-month contract. Against this benchmark, a 4,000 to 5,000 KRW adjustment to the maximum strike is about 1.1–1.4% of the payment, and a 1,000 to 1,500 KRW incentive adjustment is about 0.3–0.4%. These normalized values show that the scale guardrail primarily serves as a fine-tuning mechanism, preventing cumulative drift rather than prompting large, discrete revisions.

4.1.5 Experiment E: composite distributional alert (CDA). We evaluate joint scale and shape shocks using the composite vega index $\mathcal{V}$. Figure 4a shows that alert thresholds are crossed only when scale shocks reach $\Delta\theta/\theta = \pm 0.10$; shape shocks of similar magnitude never approach the threshold. Figure 4b confirms that, under single-shock scenarios, the scale component is the only substantive contributor to $\mathcal{V}$. Actionable alerts in this setting are therefore entirely scale-driven.

Expanding the decomposition to the full weighting grid in Eq. (20) provides a broader perspective. Figure 4c reveals widespread shape dominance across the attribution space, even though these regions do not generate alerts. This follows from two mechanisms: scale shocks determine whether an alert is triggered, while shape shocks govern attribution when valuations remain below the alert threshold.

(a) The heatmap reports the composite vega index V under joint shocks to the Weibull scale $(\Delta\theta/\theta)$ and shape $(\Delta\delta/\delta)$. Colors indicate the magnitude and sign of $\mathcal{V}$, and dashed contours mark the alert threshold defined as the 95th percentile of $|\mathcal{V}|$ across the scenario grid $(\tau \approx 0.0022)$. Alert-level responses arise only under sufficiently large scale shocks, while combinations involving smaller scale shocks or any shape shocks remain below the threshold. (b) The contribution panel decomposes $\mathcal{V}$ into its scale component C_θ and shape component C_δ for single-shock scenarios of $\pm 5\%$ in θ and δ. Only the negative scale shock produces a non-negligible response, whereas all other contributions remain effectively zero and do not trigger alerts. (c) The dominance map illustrates the relative attribution of C_θ and C_δ under alternative weighting schemes $(\omega_\theta, \omega_\delta)$. Although dominance shifts toward the shape component as ω_δ increases, this reflects attribution rather than signal strength. Even in regions of apparent δ-dominance, the composite index remains close to zero and well below the alert threshold, confirming that alert-level CDA responses are driven by scale shocks rather than shape effects.

The asymmetry is economically intuitive. Scale shocks immediately shift resale-value levels and create mark-to-market exposure, whereas shape shocks alter depreciation curvature and accumulate gradually. Thus, δ-dominance appears across large portions of the weighting map, even though curvature-driven changes seldom produce alert-level responses.

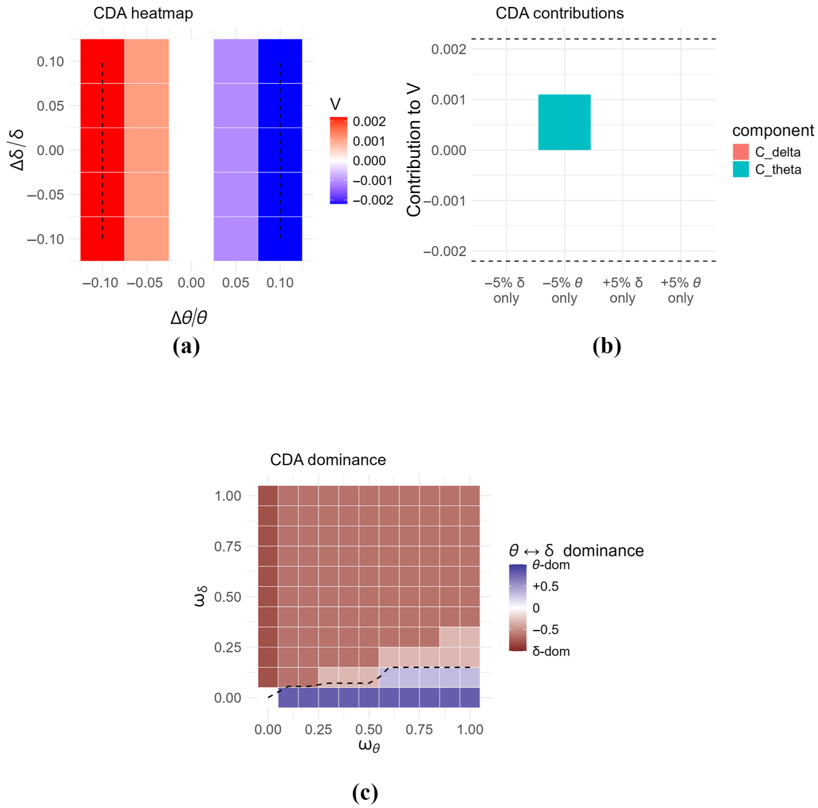

Figure 4. Composite distributional alert (CDA) analysis

From a risk-management perspective, scale shocks require immediate adjustments to guarantees or incentive guardrails. Shape sensitivity, although not alert-relevant, remains important for long-term planning and tail-risk initiatives, where curvature effects inform targeted strategic actions. The composite framework, therefore, clarifies the distinction between scale-based alert triggers and the broader dominance patterns associated with shape-driven risks.

4.2 Robustness and diagnostics

We stress-test the operating metrics using rolling-window dynamics, bootstrap uncertainty, and external validity checks. Across all exercises, the core results remain stable. Rolling estimates show gradual movements in the Weibull parameters, but these do not affect economic interpretation, and bootstrap intervals for OB, OTS, VG, and SG remain tight. The Weibull specification also consistently outperforms the lognormal and gamma benchmarks.

Figure 5a shows that δ declines from the high 11s to the mid 4s, while Figure 5b shows an increase in θ, consistent with smoother shifts in residual-value levels. The decline in δ is intuitive: nearly-new vehicles exhibit limited dispersion, whereas aging vehicles accumulate heterogeneity in mileage, usage, and condition, leading to flatter distributions. Bootstrap results confirm the precision of key KPIs. The 100-bp offset budget is tightly centered around KRW 281K, OTS remains stable near 0.358, and P_0 stays close to KRW 785K. Both the volatility and scale guardrails converge to economically meaningful ranges, indicating limited dispersion and robust calibration.

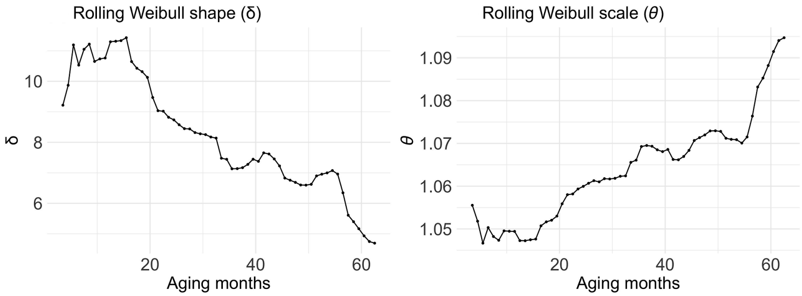

(a) **(b)**

Figure 5. Rolling Weibull parameters

This figure reports time-varying Weibull parameters estimated using a rolling window. Panel (a) shows that the shape parameter δ declines over time, implying heavier tails and greater cross-sectional dispersion in residual values. Panel (b) shows that the scale parameter θ rises gradually, indicating a shift in the distribution's central tendency.

For external validity, we apply the same procedures to the K5, Santa Fe, and Sorento. Appendix B shows closely aligned estimates and sensitivity metrics, confirming that the Weibull-based Greeks generalize across models.

Appendix C evaluates distributional fits for both the filtered and unfiltered samples. In the filtered data, the Weibull distribution yields the lowest AIC, BIC, and KS statistics and closely aligns with the QQ-plot curvature. In the unfiltered data, which contain salvage-related extremes more relevant to auto insurance than to auto finance, the Weibull specification again outperforms the lognormal and gamma benchmarks across all metrics. These results indicate that the Weibull fit remains robust even in the presence of substantial outliers.

Finally, estimating the model separately for 2020–2023 shows consistent performance across market regimes. The fit exhibits only mild deviations during the COVID shock years, a transitional pattern in 2022, and near-perfect alignment in 2023, confirming robustness under both turbulent and normalized conditions (see Appendix D).

5. Conclusion

We develop a Weibull-based framework that links residual-value risk measurement to operational decision-making in automotive finance. By translating option-theoretic sensitivities into implementable metrics such as the offset budget, offer-timing score, and guardrail adjustments, the framework supports product design, portfolio monitoring, and customer management. Evidence from Hyundai Sonata transactions shows that these tools improve decision quality under rising rate volatility and shifting market conditions, thereby connecting option-pricing theory with day-to-day managerial practice for both captive and non-captive finance providers.

The empirical results highlight structural patterns that clarify both the strengths of the framework and promising directions for further research. The Weibull distribution consistently outperforms lognormal and gamma benchmarks across filtered and unfiltered samples, underscoring its suitability for automotive-finance applications and suggesting potential relevance for settings such as auto insurance, where extreme, outlier-driven losses are economically central. These patterns also point to the potential value of extending the framework to mixture or generalized gamma variants in contexts where tail events materially influence pricing and capital allocation, consistent with recent evidence on heavy-tailed performance distributions (Lee and Lee, 2023).

Rolling-window estimates reveal systematic parameter drift, indicating that time-varying specifications merit closer study. Such extensions are increasingly important as the industry shifts from fixed maturities to subscription-based mobility models, making parameter dynamics and volatility structures central to risk management (Brown *et al.*, 2022; Weber, 2022).

Taken together, the findings establish a scalable foundation for residual-value risk analysis. Dynamic parameter extensions are most relevant for automotive finance, while enhanced tail modeling aligns more naturally with insurance settings, where extreme losses dominate.

Data availability
The dataset used in this study was obtained from the Ministry of Land, Infrastructure and Transport (MOLIT), Republic of Korea, under an academic use license. Due to licensing restrictions, the full dataset cannot be made publicly available. However, replication code and sample data supporting this study are openly available at Zenodo, https://doi.org/10.5281/zenodo.17235150. The full dataset has been made available to the editorial board and reviewers for validation purposes. Interested researchers may request access directly from MOLIT.

Acknowledgments
The author(s) gratefully acknowledge Hyundai Capital Services Korea for providing product-level profitability, market share information, and industry insights that informed the framing of this study. Although specific figures are not reported, the materials informed the broader industry context. These data are not publicly disclosed, but the author can provide the original documents, including the official company letter, upon request.

Supplementary material
The supplementary material for this article can be found online.

References

Belzowski, B. (2009), "Can Chrysler survive its reinvention?", in *The Second Automobile Revolution: Trajectories of the World Carmakers in the 21st Century*, Palgrave Macmillan UK, London, pp. 206-222.

Brown, C., Hardman, M., Davies, N. and Armitage, R. (2022), "Mobility as a service: defining a transport utopia", *Future Transport*, Vol. 2 No. 1, pp. 300-309, doi: 10.3390/futuretransp2010016.

Eurofinas (2024), "Annual conventions 2024 report", Eurofinas, available at: https://www.eurofinas.org/_flysystem/s3?file=ANNUAL_CONVENTIONS_2024_Report_.pdf

Federal Reserve Bank of St. Louis (2025), "Consumer motor vehicle leases owned by finance companies", [DTCORVHFNM]. FRED, Federal Reserve Bank of St. Louis, available at: https://fred.stlouisfed.org/series/DTCORVHFNM

Gamba, A. and Rigon, R. (2008), "The value of embedded real options: evidence from consumer automobile lease contracts–a note", *Finance Research Letters*, Vol. 5 No. 4, pp. 213-220, doi: 10.1016/j.frl.2008.08.003.

Giaccotto, C., Goldberg, G.M. and Hegde, S.P. (2007), "The value of embedded real options: evidence from consumer automobile lease contracts", *Journal of Finance*, Vol. 62 No. 1, pp. 411-445, doi: 10.1111/j.1540-6261.2007.01211.x.

Hariri, S., Kind, M.C. and Brunner, R.J. (2019), "Extended isolation forest", *IEEE Transactions on Knowledge and Data Engineering*, Vol. 33 No. 4, pp. 1479-1489, doi: 10.1109/TKDE.2019.2947676.

Ko, S.B. (2025), "Real option valuation using Weibull distribution: a new framework for depreciation risk management", *Journal of Derivatives and Quantitative Studies: 선물연구*, Vol. 33 No. 2, pp. 110-130, doi: 10.1108/JDQS-10-2024-0041.

Lee, J. and Lee, C. (2023), “The performance distribution and managerial skill of passive funds: evidence from the Korean market”, *Journal of Derivatives and Quantitative Studies: 선물연구*, Vol. 31 No. 4, pp. 328-346, doi: 10.1108/JDQS-05-2023-0009.

Li, K. and You, L. (2022), “Flexibility, option value of leasing, and investment”, *SSRN*, doi: 10.2139/ssrn.4381925.

McConnell, J.J. and Schallheim, J.S. (1983), “Valuation of asset leasing contracts”, *Journal of Financial Economics*, Vol. 12 No. 2, pp. 237-261, doi: 10.1016/0304-405X(83)90037-5.

Miller, S.E. (1995), “Economics of automobile leasing: the call option value”, *Journal of Consumer Affairs*, Vol. 29 No. 1, pp. 199-218, doi: 10.1111/j.1745-6606.1995.tb00045.x.

Mordor Intelligence (2025), *South Korea Electric Vehicle Leasing Market Size & Share Analysis - Growth Trends and Forecast (2025-2030)*, Mordor Intelligence, available at: https://www.mordorintelligence.com/industry-reports/south-korea-electric-vehicle-leasing-market

Oppenheimer, P. (2002), “Including real options in evaluating terminal cash flows in consumer auto leases”, *Financial Services Review*, Vol. 11 No. 2, pp. 135-151.

Park, C. and Padgett, W.J. (2006), “Stochastic degradation models with several accelerating variables”, *IEEE Transactions on Reliability*, Vol. 55 No. 2, pp. 379-390, doi: 10.1109/TR.2006.874937.

Rousseeuw, P.J. (1987), “Silhouettes: a graphical aid to the interpretation and validation of cluster analysis”, *Journal of Computational and Applied Mathematics*, Vol. 20, pp. 53-65, doi: 10.1016/0377-0427(87)90125-7.

Steinley, D. and Brusco, M.J. (2007), “Initializing K-means batch clustering: a critical evaluation of several techniques”, *Journal of Classification*, Vol. 24 No. 1, pp. 99-121, doi: 10.1007/s00357-007-0003-0.

Trigeorgis, L. (1996), “Evaluating leases with complex operating options”, *European Journal of Operational Research*, Vol. 91 No. 2, pp. 315-329, doi: 10.1016/0377-2217(95)00288-X.

Weber, J. (2022), “Mobility as a service”, in *Moving Times*, Springer, Wiesbaden, pp. 161-228, doi: 10.1007/978-3-658-37733-5_5.

Weibull, W. (1951), “A statistical distribution function of wide applicability”, *Journal of Applied Mechanics*, Vol. 18 No. 3, pp. 293-297, doi: 10.1115/1.4010337.

Ye, Z.S. and Chen, N. (2014), “The inverse Gaussian process as a degradation model”, *Technometrics*, Vol. 56 No. 3, pp. 302-311, doi: 10.1080/00401706.2013.830074.

Corresponding author
Seok Bin Ko can be contacted at: Sbko@cju.ac.kr